Electronic Supplementary Material (ESI) for Materials Chemistry Frontiers.

Supporting Information

Intrinsic conductivity optimization of bi-metallic nickel cobalt selenides toward superior-rate Na-ion storage

Chen Wu, [a] Yuehua Wei, [a] Qingwang Lian, [a] Chao Cui, [a] Weifeng Wei, [a] Libao Chen*[a] and Chengchao Li* [b]

[a] State Key Laboratory of Powder Metallurgy, Central South University, Changsha 410083, China.

[b] School of Chemical Engineering and Light Industry, Guangdong University of Technology, Guangzhou 510006, China.

*To whom correspondence should be addressed: lbchen@csu.edu.cn and licc@gdut.edu.cn

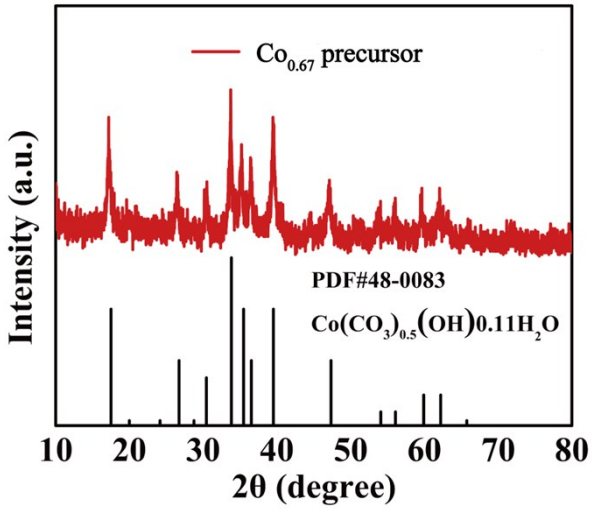

Fig. S1 XRD pattern of the precursor of $Co_{0.67}$

The diffraction peaks could be matched with the peaks of $Co(CO_3)_{0.5}(OH)0.11H_2O$ (PDF#48-0083) with the exception that all peaks shift lightly to lower angle due to the partial substitution of Ni for Co.

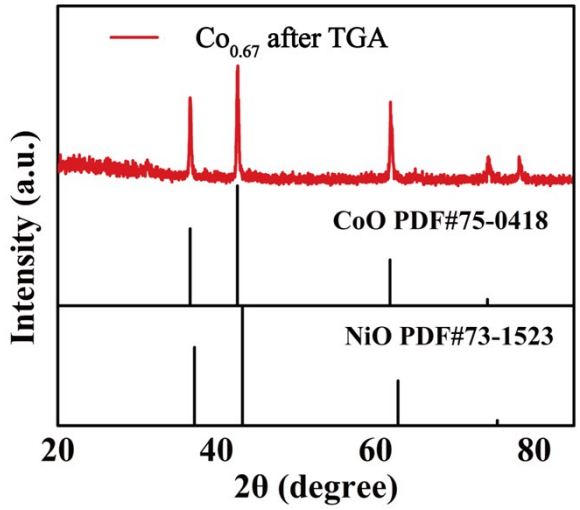

Fig. S2 XRD pattern of the final product after annealing at 1000 ^{o}C for $Co_{0.67}$.

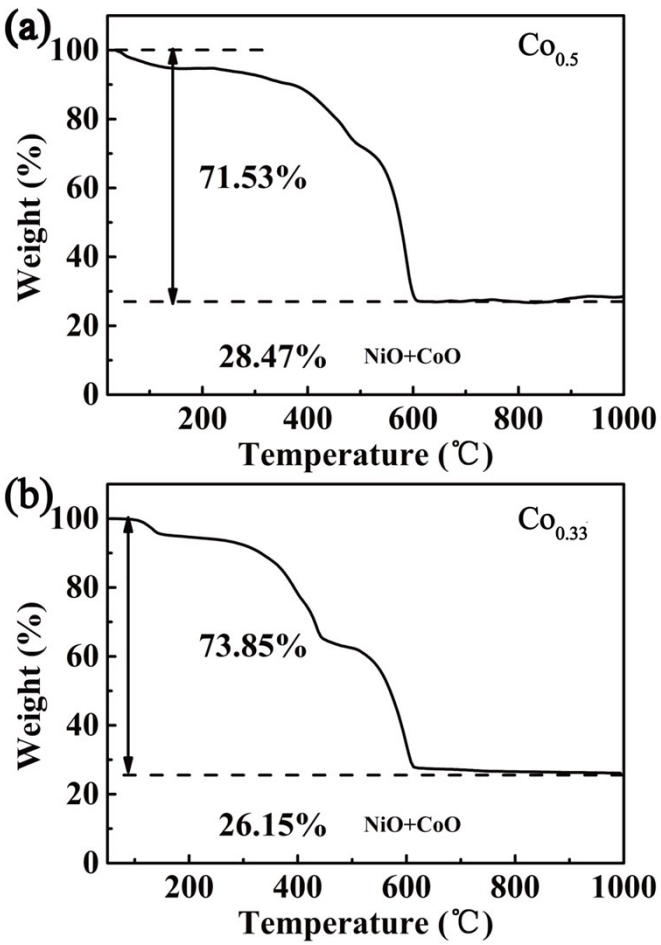

Fig. S3 TGA of (a) $Co_{0.5}$ (b) $Co_{0.33}$ from room temperature to 1000 ^{o}C at ramping rate of 10 ^{o}C min^{-1} in air.

The final products are indexed as NiO (PDF#44-1159) and CoO (PDF#70-2855). The two oxides has similar relative molar mass (74.69 for NiO and 74.93 for CoO), so we use the average (74.81) to calculate the mass raito. According to Equation S1 and S2, the final carbon contents can be calculated as 20.2, 17.5 and 24.2 wt. % for $Co_{0.67}$, $Co_{0.5}$ and $Co_{0.33}$, respectively.

$$Ni_xCo_{1-x}Se_2 + O_2 \rightarrow x\ NiO + (1-x)\ CoO + SeO_2 \qquad S1$$

$$W_c = 1 - (78.96 * 2 * W_1 / 74.81 + 58.81 * W_1 / 74.81) \qquad S2$$

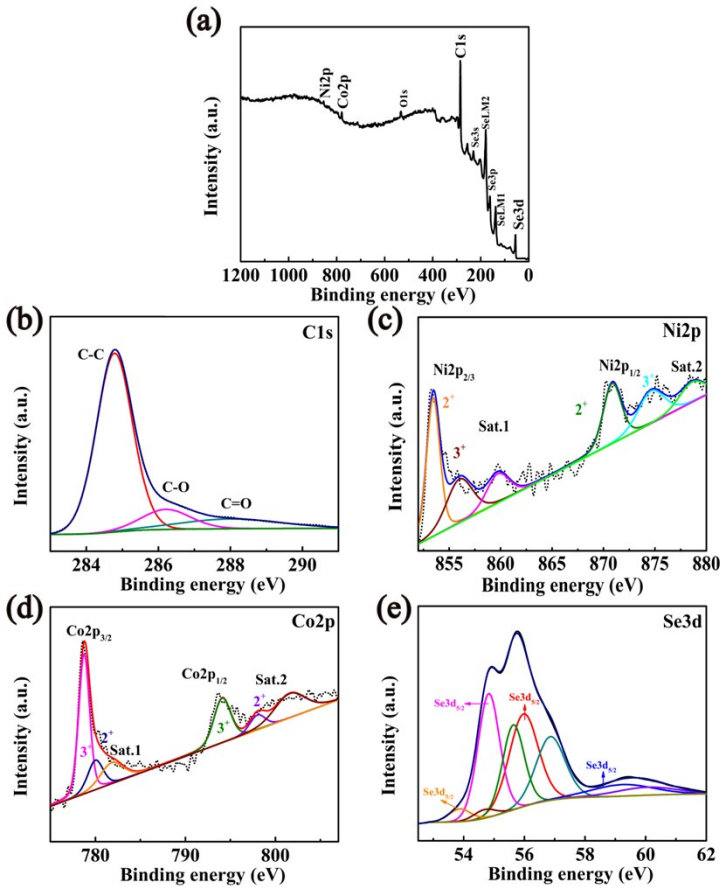

Fig. S4 XPS spectra of $Co_{0.67}$ (a) Survey spectrum, (b) C 1s, (c) Ni 2p, (d) Co 2p and (e) Se 3d.

The survey spectrum (Fig. S4a) indicates that the main elements present in the sample are C, Ni, Co, Se and O, and the presence of O is attributed to the oxidation of the sample for long time in air. All peaks were fitted by typical Gauss Lorentz equation. The high resolution spectrum of C (Fig. S4b) derived from CNF and C layer could be fitted into three peaks classified as C-C (284.78 eV), C-O (286.21 eV) and C=O (287.99 eV),[1, 2] respectively. The spectrum of Ni 2p (Fig. S4c) encompasses two peaks centered at 853.41 eV (Ni 2p3) and 870.84 eV (Ni 2p1) that belong to Ni^{2+} and another two peaks located in 856.00 eV (Ni 2p3) and 874.63 eV (Ni 2p1) that are assigned to Ni^{3+}.[3-5] The peaks situated at 778.74 eV (Co 2p3) and 794.06 eV (Co 2p1)

(Fig. S4d) are ascribed to Co^{3+} while the other two peaks with the binding energy of 780.00 eV (Co 2p3) and 797.94 eV (Co 2p1) are identified as Co^{2+}.[6] The fitted peaks of Se ((Fig. S4e) are a little complex, in which seated at 54.83 eV (Se 3d5) is deemed to the combination with Ni and Co,[7] located in 55.97 eV (Se 3d5) may be due to the tight integration with carbon,[8] and centered at 59.23 eV (Se 3d5) is originated from the presence of SeO_2, slight oxidization of the surface in air.[6]

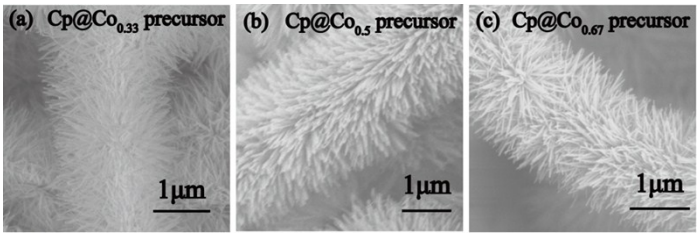

Fig. S5 SEM images of (a) $Co_{0.33}$, (b) $Co_{0.5}$ and (c) $Co_{0.67}$ precursors after carbon coating.

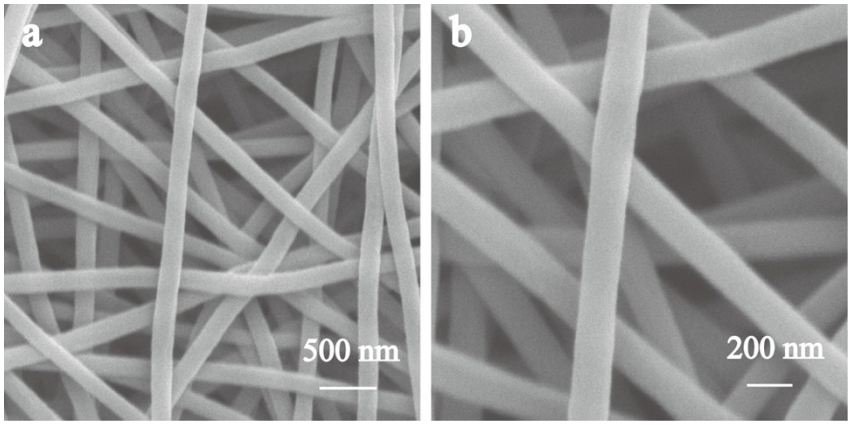

Fig. S6 SEM images of the substrate C nanofibers (CNFs)

The smaller diameter of CNF is around 200 nm. Relative to carbon cloth (several micrometers), CNF could provide larger mass loading.[9]

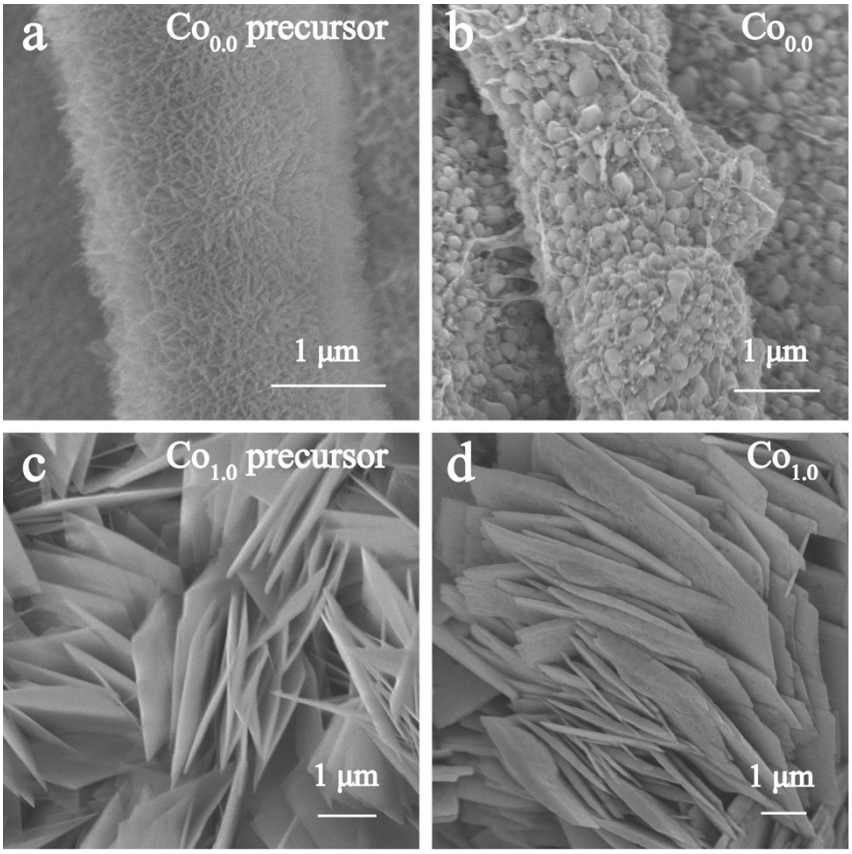

Fig. S7 SEM images of the (a) $Co_{0.0}$ precursor, (b) $Co_{0.0}$, (c) $Co_{1.0}$ precursor and (d) $Co_{1.0}$

The precursor of pure $NiSe_2$ (Fig. S7a) has denser nanoneedles (more like fluff) on CNF and fusing together into coadjacent particles coated on CNF during selenization (Fig. S7b), sparing almost a little space for volume expansion. Nevertheless the nanoplates of pure $Co_{1.0}$ precursor (Fig. S7c) are separate from CNF and distribute as clusters, so the resulting $CoSe_2$ (Fig. S7d) possesses the alike morphology of nanoplates. An interesting phenomenon is observed that from the view of the morphology of precursors, bimetallic precursors are prone to come into being the alike morphology of pure $Co_{0.0}$ precursor.

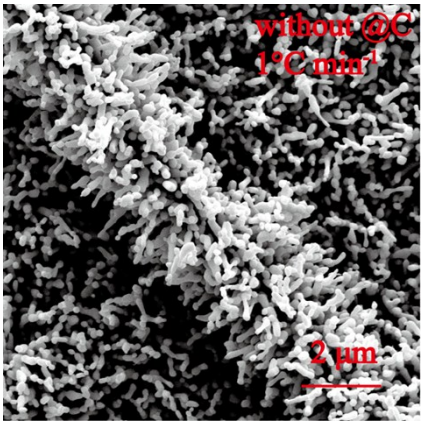

Fig. S8 SEM image of the $Ni_{0.33}Co_{0.67}Se_2$/CNF without carbon coating at 1 ^oC min^{-1}

The morphology changed a lot in the shape and diameter of the nanorods which may originate from the adjacent particles fusing together without carbon protection.

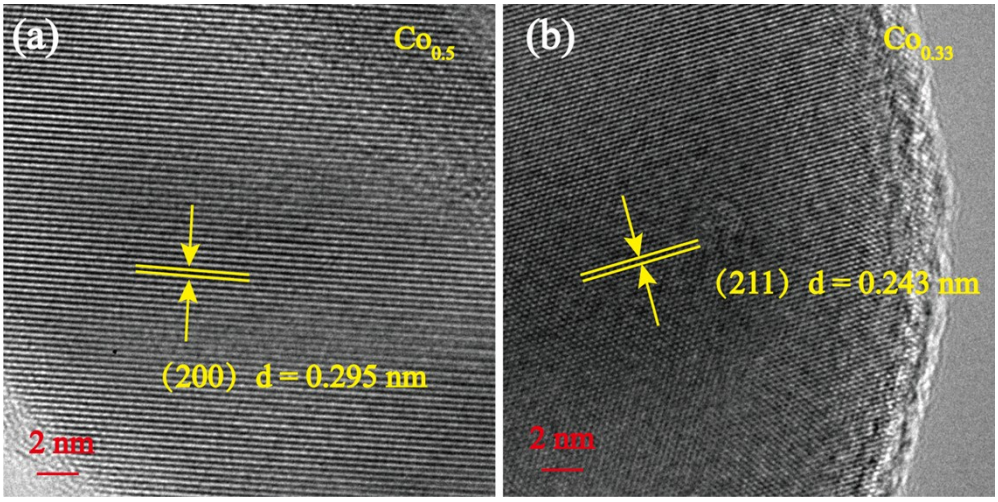

Fig. S9 HRTEM images of (a) $Co_{0.5}$ and (b) $Co_{0.33}$

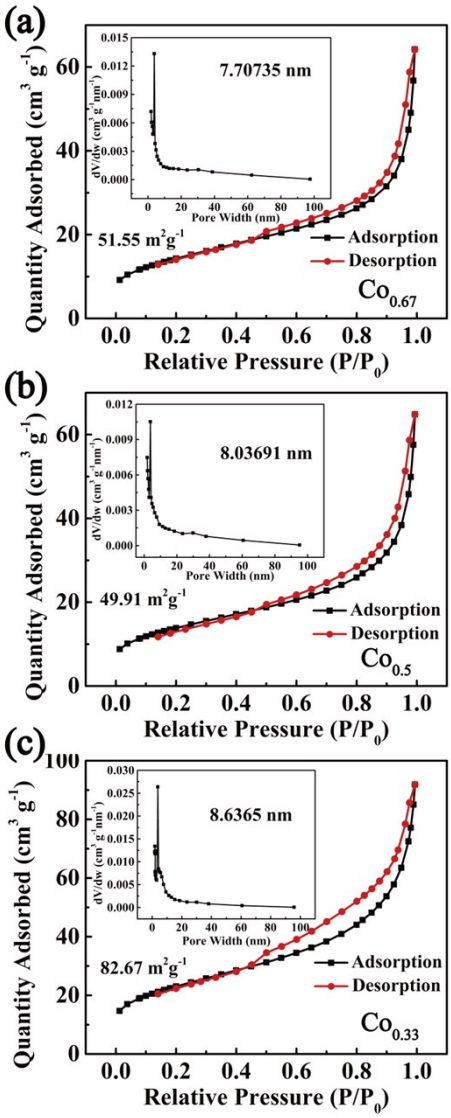

Fig. S10 N_2 adsorption-desorption isotherms of (a) $Co_{0.67}$, (b) $Co_{0.5}$, (c) $Co_{0.33}$

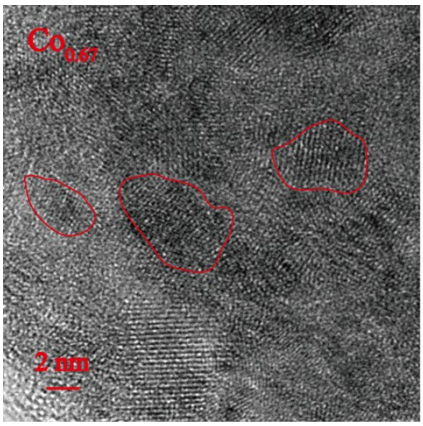

Fig. S11 HRTEM of $Co_{0.67}$ after first cycle.

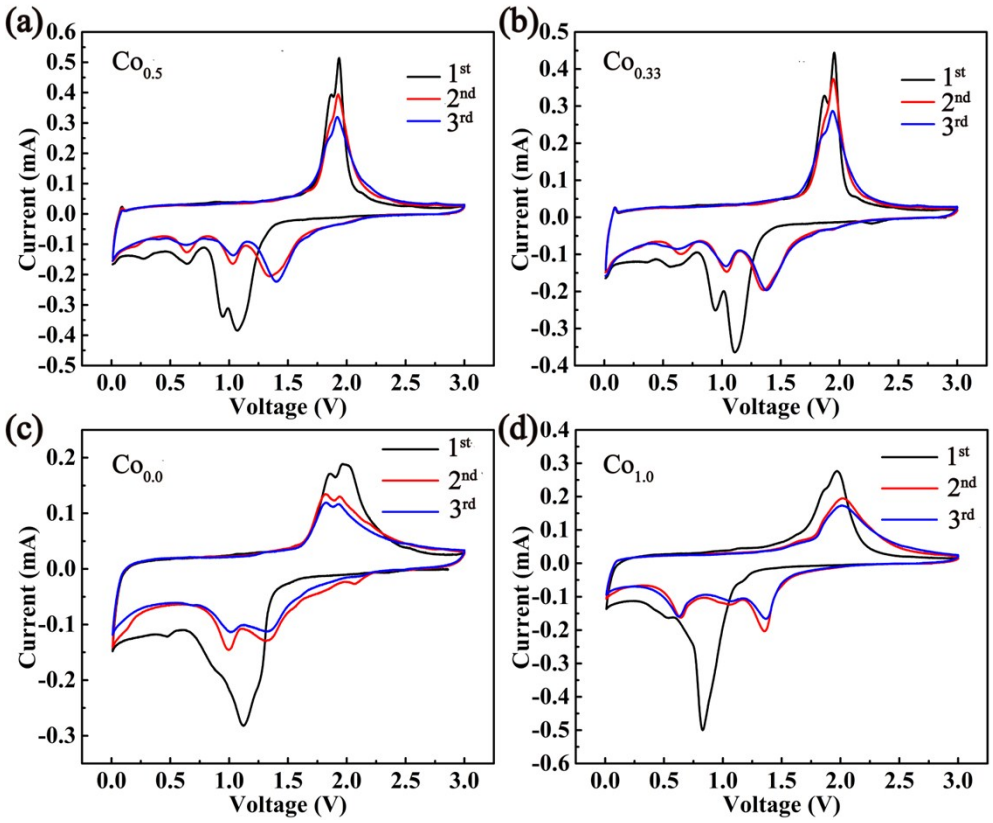

Fig. S12 The cyclic voltammetry curves of (a) $Co_{0.5}$, (b) $Co_{0.33}$, (c) $Co_{0.0}$ and (d) $Co_{1.0}$.

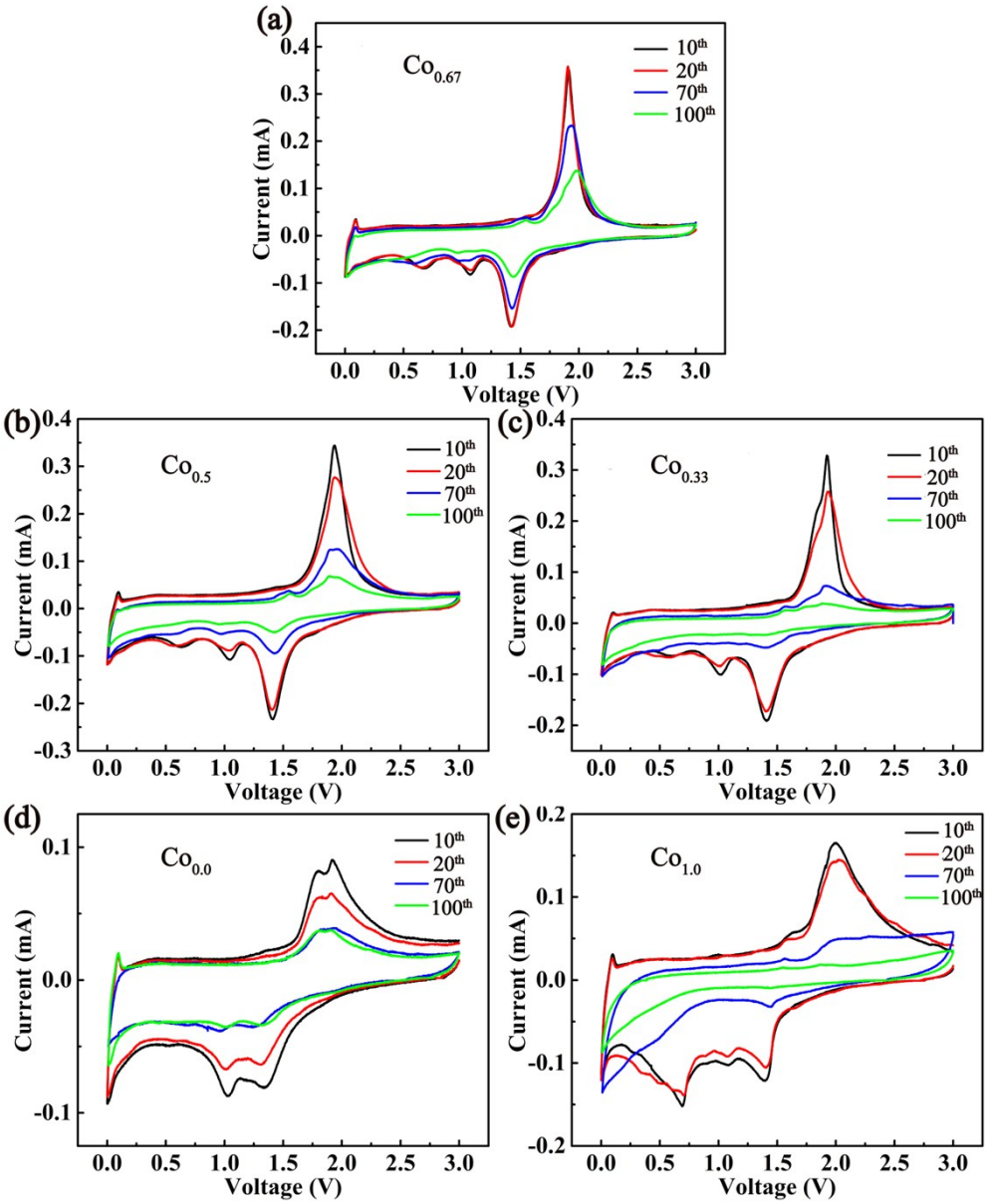

Fig. S13 The cyclic voltammetry curves with different cycles of (a) $Co_{0.67}$, (b) $Co_{0.5}$, (c) $Co_{0.33}$, (d) $Co_{0.0}$ and (e) $Co_{1.0}$.

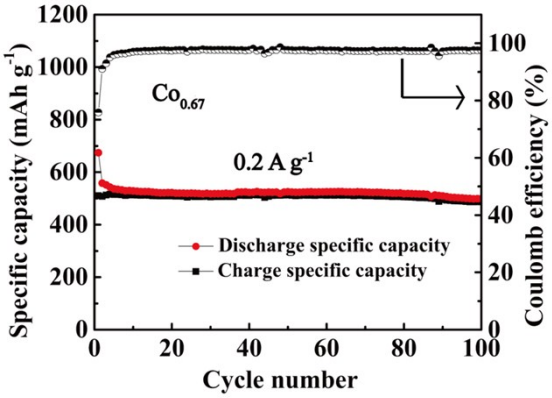

Fig. S14 The cycling performance and coulomb efficiency of $Co_{0.67}$.

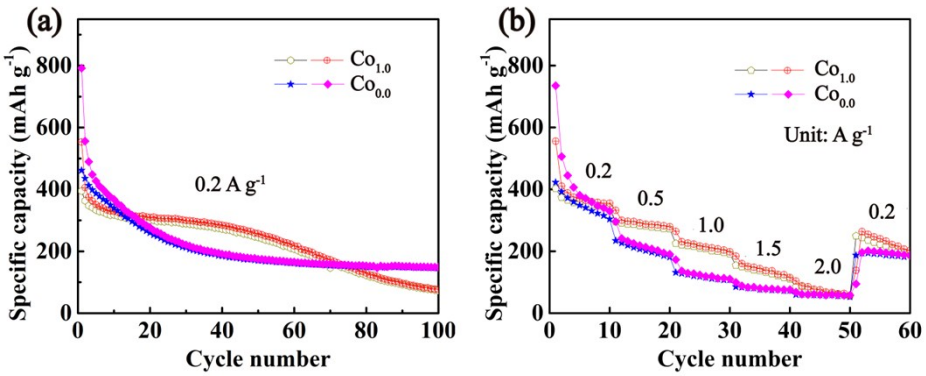

Fig. S15 (a) The cycle performance and (b) rate performance of $Co_{0.0}$ and $Co_{1.0}$ as anode for NIBs

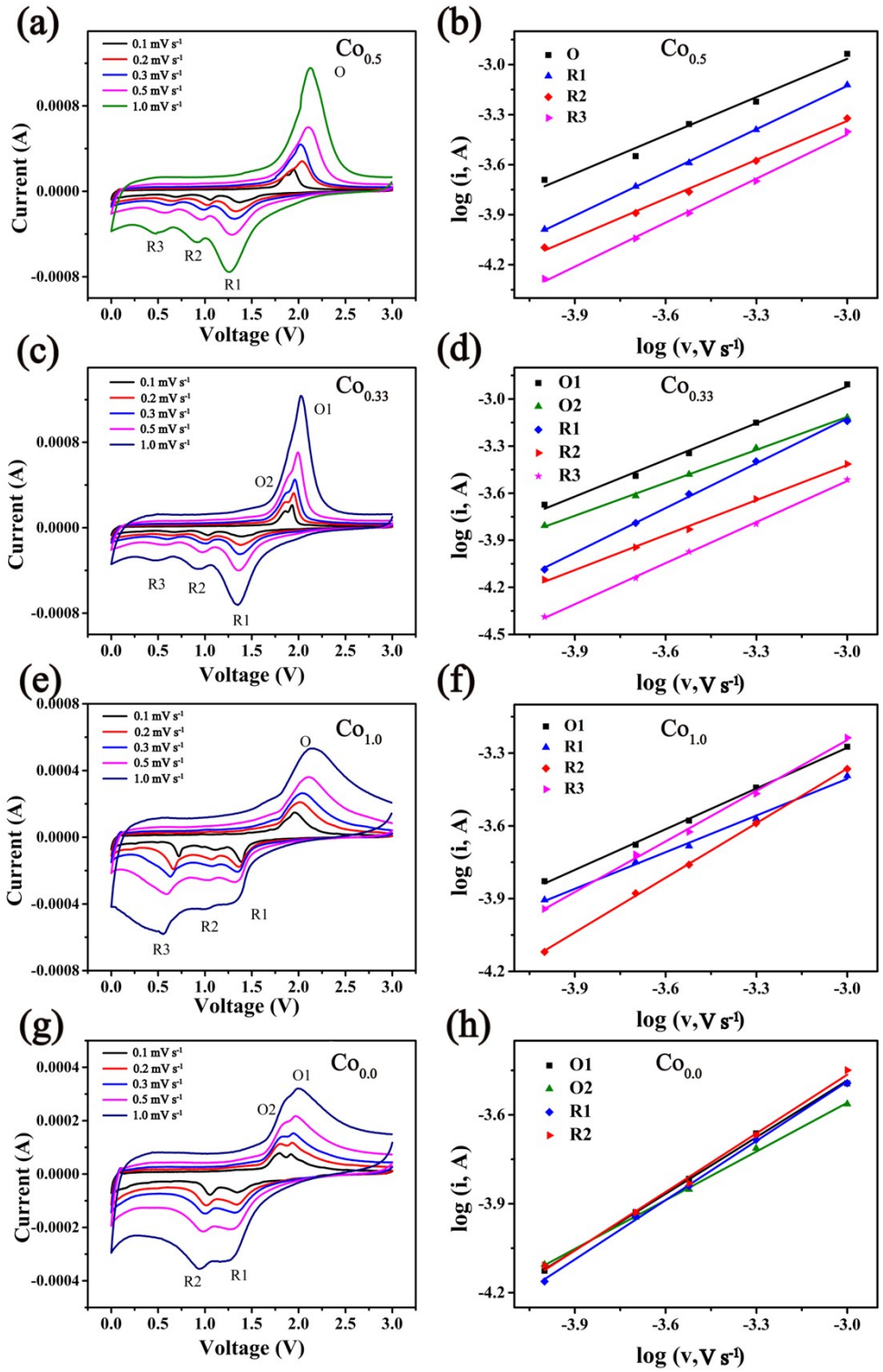

Fig. S16 The cyclic voltammetry curves with different scan rates in the voltage range of 0.01-3 V (left) and log (i) vs. log (v) plots at each redox peak (right) of C@$Ni_xCo_{1-x}Se_2$/CNF composites, where (a, b) x = 0.5, (c, d) x = 0.67, (e, f) x = 0, and (g, h) x = 1.

Table S1 ICP results of the molar ratio of $Co_{0.33}$, $Co_{0.5}$ and $Co_{0.67}$

Ratio	Molar ratio		
	$Co_{0.33}$	**$Co_{0.5}$**	**$Co_{0.67}$**
Co/(Co + Ni)	0.34	0.51	0.66
Se/(Co + Ni)	1.96	1.97	1.96

Table S2 The fitting parameters of $Co_{0.67}$, $Co_{0.5}$ and $Co_{0.33}$ on EIS

Material	R_s	R_{ct}	**$Co_{0.67}$ Cycles**	R_s	R_{ct}
$Co_{0.67}$	6.4	225.5	10	8.5	138.0
$Co_{0.5}$	5.9	328.5	30	9.7	92.1
$Co_{0.33}$	10.4	374.0	50	7.4	74.2

Table S3 The b values at each redox peak of five composites

Material	O1	O2	R1	R2	R3
$Co_{1.0}$	0.56	-	0.50	0.75	0.70
$Co_{0.67}$	0.83	-	0.95	0.76	0.88
$Co_{0.5}$	0.76	-	0.86	0.78	0.88
$Co_{0.33}$	0.78	0.70	0.95	0.74	0.87
$Co_{0.0}$	0.64	0.55	0.67	0.66	-

1. I. H. Kwak, H. S. Im, D. M. Jang, Y. W. Kim, K. Park, Y. R. Lim, E. H. Cha and J. Park, *ACS applied materials & interfaces*, 2016, **8**, 5327-5334.
2. J. S. Cho, S. Y. Lee and Y. C. Kang, *Scientific reports*, 2016, **6**, 23338.
3. Z. Liu, X. Zheng, S.-l. Luo, S.-q. Xu, N.-y. Yuan and J.-n. Ding, *J. Mater. Chem. A*, 2016, **4**, 13395-13399.
4. Y. Ruan, J. Jiang, H. Wan, X. Ji, L. Miao, L. Peng, B. Zhang, L. Lv and J. Liu,

Journal of Power Sources, 2016, **301**, 122-130.

5. Y. Ge, S. P. Gao, P. Dong, R. Baines, P. M. Ajayan, M. Ye and J. Shen, *Nanoscale*, 2017.
6. X. Qian, H. Li, L. Shao, X. Jiang and L. Hou, *ACS applied materials & interfaces*, 2016, **8**, 29486-29495.
7. D. Kong, H. Wang, Z. Lu and Y. Cui, *Journal of the American Chemical Society*, 2014, **136**, 4897-4900.
8. Y. Jiang, X. Ma, J. Feng and S. Xiong, *J. Mater. Chem. A*, 2015, **3**, 4539-4546.
9. Y. Wei, F. Yan, X. Tang, Y. Luo, M. Zhang, W. Wei and L. Chen, *ACS applied materials & interfaces*, 2015, **7**, 21703-21711.